Acta Crystallographica Section B
Structural Science
ISSN 0108-7681

Monitoring structural transformations in crystals. 8. Monitoring molecules and a reaction center during a solid-state Yang photocyclization

Ilona Turowska-Tyrk,[a]* Elżbieta Trzop,[a] John R. Scheffer[b] and Shuang Chen[b]

[a]Department of Chemistry, Wrocław University of Technology, Wybrzeże Wyspiańskiego 27, 50-370 Wrocław, Poland, and [b]Department of Chemistry, University of British Columbia, 2036 Main Mall, Vancouver, British Columbia, Canada V6T 1Z1

Correspondence e-mail: ilona.turowska-tyrk@pwr.wroc.pl

Received 6 July 2005
Accepted 20 October 2005

Structural changes taking place in a crystal during an intramolecular photochemical reaction [the Yang photocyclization of the α-methylbenzylamine salt with 1-(4-carboxybenzoyl)-1-methyladamantane] were monitored step-by-step using X-ray structure analysis. This is the first example of such a study carried out for an intramolecular photochemical reaction. During the photoreaction, both the reactant and product molecules change their orientation, but the reactant changes more rapidly after the reaction is about 80% complete. The distance between directly reacting atoms in the reactant molecule is almost constant until about 80% reaction progress and afterwards decreases. The torsion angle defined by the reactant atoms that form the cyclobutane ring also changes in the final stages of the photoreaction. These phenomena are explained in terms of the influence of many product molecules upon a small number of reacting molecules. The adamantane portion shifts more than the remaining part of the anionic reactant species during the reaction, which is explained in terms of hydrogen bonding. The structural changes are accompanied by changes in the cell constants. The results obtained in the present study are compared with analogous results published for intermolecular reactions.

1. Introduction

Interest in the photochemical reactions of crystals has been strong for many years and has recently increased significantly. A variety of techniques have been applied to studies in this field (Boldyreva, 1999) and among them X-ray structure analysis is one of the most effective. In recent years, papers on monitoring structural changes in crystals during photochemical reactions by means of X-ray structure analysis have started to appear (Fernandes & Levendis, 2004; Ohba & Ito, 2003; Turowska-Tyrk, 2001, 2003, 2004; Turowska-Tyrk & Trzop, 2003). The above-mentioned papers deal with intermolecular reactions, namely [2 + 2] and [4 + 4] photodimerizations, and describe the movements of the reactant and product molecules during reaction. X-ray structural studies of intramolecular photochemical reactions in crystals have also been reported. Structures of partly reacted crystals, *i.e.* crystals containing both reactant and product molecules, have appeared, but they serve mainly as evidence for reactions occurring in crystals or as an explanation of the reaction mechanism (Harada *et al.*, 1999; Hosomi *et al.*, 2000; Leibovitch *et al.*, 1997, 1998; Ohba *et al.*, 2000; Patrick *et al.*, 2003*a*,*b*; Yamamoto *et al.*, 2003*a*,*b*). Here we present a study of the intramolecular Yang photocyclization of (1) presented in (I) (Leibovitch *et al.*, 1997, 1998). Compound (1) is a salt consisting of cationic and anionic chemical species. Only one of the species, the anion, takes part directly in the photo-

reaction. As can be seen, during the reaction a new intramolecular bond is created and as a result a cyclobutane ring is formed. The advantage of this photoreaction is that it proceeds in a single-crystal to single-crystal way (Leibovitch *et al.*, 1997, 1998). Such a feature enables the monitoring of structural changes during the 'reactant crystal–product crystal' transformation. Monitoring studies for the salt presented in (I) are interesting, since they can reveal not only the behavior of the reacting anionic species, but also the behavior of the cationic species, which is an unreactive 'bystander'.

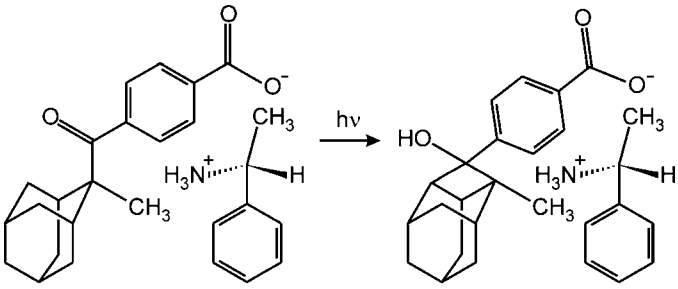

(1) (I)

2. Experimental

Compound (1) was synthesized by the method described by Leibovich *et al.* (1998). All the X-ray experiments were carried out on the same crystal. The crystal was irradiated in steps using a Hg 100 W lamp and a WG-320 glass filter (the filter transmitted longer wavelengths and blocked shorter wavelengths: 0% transmittance for $\lambda < 300$ nm, *ca* 95% transmittance at 350 nm and 100% transmittance for $\lambda > 365$ nm). The lengths of time of irradiation were 2.5, 5, 8, 12, 16, 20, 28, 36, 45, 55, 70 and 90 min. The direction of the irradiation beam was always perpendicular to the longest crystal dimension. The crystal was rotated during the irradiation. Our estimates indicate that for wavelengths in the absorption maximum, almost all light would be absorbed in the first 0.07 mm of the crystal. Owing to this, the beam filtered by the WG-320 glass filter mentioned above, *i.e.* the beam containing longer (and more weakly absorbed by the reactant) wavelengths, was used. Then the crystal penetration was much better and the reaction throughout the crystal was much more random. It should be added that the photoproduct did not absorb significantly at the irradiation wavelengths which were used. Moreover, the thinness of the crystal, the direction of the irradiation (perpendicular to the longest crystal dimension) and rotation of the crystal during the irradiation also helped improve crystal penetration. After each step of the irradiation, X-ray data were collected and the crystal structure determined. The intensities of the reflections were collected by means of a diffractometer equipped with a CCD detector. The general strategy for data collection for area-detector diffractometers was described by Scheidt & Turowska-Tyrk (1994). The cell constants were determined on the basis of a representative fraction of the reflections (Kuma Diffraction, 2000). There were no problems with determinations of unit-cell constants. For all steps of the photoreaction, including the pure product crystal, the per cent of reflections for which the positions were predicted well by the orientation matrix was almost constant; the biggest difference was 4%. This fit would indicate that the photoreaction has features of a random reaction and that at no time was the crystal composed of macroscopic regions of separated reactant and product. The collected data were corrected for Lorentz and polarization effects (Kuma Diffraction, 2000). The structures were refined by means of *SHELXL*97 (Sheldrick, 1997). Structures of pure reactant, pure product and one mixed reactant–product crystal have been published previously (Leibovitch *et al.*, 1997, 1998). Atomic coordinates published for the pure component crystals, available in the Cambridge Structural Database (refcodes NIHCUC and NIHDAJ) have been used here as the input for our pure product crystal and the non-irradiated crystal. For the pure product crystal, non-H atoms were refined anisotropically; H atoms were found in a ΔF map, but most of them were refined with constraints. For intermediate stages of the photoreaction for which the reactant was the major component, initial atomic coordinates for the reactant were taken from the non-irradiated crystal and the first atoms of the product were found in ΔF maps, the positions of the remaining atoms being calculated geometrically. For the mixed crystals, the major component was refined anisotropically and the minor one isotropically, except for the crystals of 42.3% reaction progress and 51.8% reaction progress, where both components were refined anisotropically. The positions of the H atoms for the partly reacted crystals were calculated geometrically and refined with constraints. The reactant–product disorder, which is a feature of mixed crystals, required the use of many constraints and restraints of thermal and geometrical parameters. It is also likely that the reactant and the product molecules are not equally and regularly arranged in the unit cells. The following options from *SHELXL*97 (Sheldrick, 1997) were applied: DFIX, DANG, FLAT, AFIX and SIMU for all mixed crystals and additionally ISOR for the 42.3 and 51.8% product crystals. The percentage of the reactant (and of the product) in the crystal was determined during the refinements. The time necessary for one crystal structure determination varied from one to several days. It should be added that the crystal structure at each stage of the photoreaction is a static average of a mixed crystal composed of the reactant and the product, and that no intermediate was ever observed. Selected experimental data are given in Table 1 for three of the refinements (at 26.5, 42.3 and 87.5% of the product); data for all refinements (at 4.4, 10.6, 26.5, 42.3, 51.8, 74.5, 80.1, 87.5, 91.0, 94.5, 95.8, 96.2 and 100% of the product) are given in the supplementary material.[1] It is our routine to always check during photo-induced experiments to see whether the reaction occurs in the absence of radiation from a UV–vis lamp. In order to check this for the examined

[1] Supplementary data for this paper are available from the IUCr electronic archives (Reference: BK5019). Services for accessing these data are described at the back of the journal.

Table 1
Experimental details.

Selected data only - the full data are available in the cif.

	26.5%*P*	42.3%*P*	87.5%*P*
Crystal data			
Chemical formula	$C_{27}H_{33}NO_3$	$C_{27}H_{33}NO_3$	$C_{27}H_{33}NO_3$
M_r	419.54	419.54	419.54
Cell setting, space group	Orthorhombic, $P2_12_12_1$	Orthorhombic, $P2_12_12_1$	Orthorhombic, $P2_12_12_1$
a, b, c (Å)	11.8470 (13), 29.649 (3), 6.5443 (6)	11.8971 (15), 29.579 (3), 6.5350 (7)	12.364 (3), 28.956 (6), 6.4582 (11)
V (Å^3)	2298.7 (4)	2299.7 (4)	2312.1 (8)
Z	4	4	4
D_x (Mg m^{-3})	1.212	1.212	1.205
Radiation type	Mo $K\alpha$	Mo $K\alpha$	Mo $K\alpha$
No. of reflections for cell parameters	1918	1628	1451
θ range (°)	6–19	6–19	6–19
μ (mm^{-1})	0.08	0.08	0.08
Temperature (K)	293 (2)	293 (2)	293 (2)
Crystal form, colour	Block, colourless	Block, colourless	Block, colourless
Crystal size (mm)	0.56 × 0.41 × 0.20	0.56 × 0.41 × 0.20	0.56 × 0.41 × 0.20
Data collection			
Diffractometer	Kuma KM4CCD	Kuma KM4CCD	Kuma KM4CCD
Data collection method	ω scans	ω scans	ω scans
Absorption correction	None	None	None
No. of measured, independent and observed reflections	10 623, 3972, 3083	10 696, 3986, 2925	10 478, 3996, 3001
Criterion for observed reflections	$I > 2\sigma(I)$	$I > 2\sigma(I)$	$I > 2\sigma(I)$
R_{int}	0.071	0.089	0.078
θ_{max} (°)	25.0	25.0	25.0
Range of h, k, l	$-13 \Rightarrow h \Rightarrow 14$ $-35 \Rightarrow k \Rightarrow 35$ $-7 \Rightarrow l \Rightarrow 6$	$-14 \Rightarrow h \Rightarrow 13$ $-35 \Rightarrow k \Rightarrow 35$ $-6 \Rightarrow l \Rightarrow 7$	$-13 \Rightarrow h \Rightarrow 14$ $-34 \Rightarrow k \Rightarrow 34$ $-6 \Rightarrow l \Rightarrow 7$
Refinement			
Refinement on	F^2	F^2	F^2
$R[F^2 > 2\sigma(F^2)]$, $wR(F^2)$, S	0.083, 0.208, 1.08	0.085, 0.218, 1.06	0.088, 0.230, 1.11
No. of reflections	3972	3986	3996
No. of parameters	406	561	406
H-atom treatment	Constrained to parent site	Constrained to parent site	Constrained to parent site
Weighting scheme	$w = 1/[\sigma^2(F_o^2) + (0.0806P)^2 + 1.2849P]$, where $P = (F_o^2 + 2F_c^2)/3$	$w = 1/[\sigma^2(F_o^2) + (0.0901P)^2 + 1.1566P]$, where $P = (F_o^2 + 2F_c^2)/3$	$w = 1/[\sigma^2(F_o^2) + (0.0849P)^2 + 1.6461P]$, where $P = (F_o^2 + 2F_c^2)/3$
$(\Delta/\sigma)_{max}$	0.001	0.002	0.002
$\Delta\rho_{max}$, $\Delta\rho_{min}$ (e Å^{-3})	0.20, −0.16	0.18, −0.17	0.24, −0.21
Extinction method	*SHELXL*	*SHELXL*	*SHELXL*
Extinction coefficient	0.087 (12)	0.094 (14)	0.093 (13)
Absolute configuration	The absolute configuration was assigned to agree with that from Leibovitch *et al.* (1997, 1998) by taking the same enantiomer of the cation	The absolute configuration was assigned to agree with that from Leibovitch *et al.* (1997, 1998) by taking the same enantiomer of the cation	The absolute configuration was assigned to agree with that from Leibovitch *et al.* (1997, 1998) by taking the same enantiomer of the cation

Computer programs used: *KM4CCD* (Kuma Diffraction, 2000), *SHELXL*97 (Sheldrick, 1997), *ORTEP*3 (Farrugia, 1997).

compound, two additional data sets were collected: the first immediately after irradiation of a crystal and the second data set after 1 d. The content of the product determined was statistically the same for both cases; the difference was smaller than half a standard deviation. It is also our routine to carry out all experiments in the dark. The structure determination process also confirmed that crystals of the examined compound were not sensitive to X-rays.

3. Results and discussion

The change of percentage product content in a crystal, P, with time of irradiation, t, is shown in Fig. 1. The dependence is well described by the following exponential function

$$P = 100 - 101\,(3)\exp[(-t/14.0\,(8)],$$

with a correlation coefficient of 0.994; the numbers in parentheses are standard uncertainties for the last digits. As shown in Fig. 1, during the first 20 min of irradiation, the progress of the photoreaction is rapid, ∼ 80%, and during the next 70 min the remaining 20% of the product is formed. Nevertheless, our studies have revealed that during the final 20% of the reaction progress, the changes in the crystal structure are large. Fig. 2 presents the variation of the cell constants with the product content in a crystal. As can be seen, a and b change much faster during the final stages of the photoreaction than at the beginning. A similar but less pronounced trend can also be observed for the c constant. The

unit-cell volume changes in an interesting way: after a prolonged increase, it decreases quickly in the final stages of the photoreaction. In the case of the [2 + 2] photodimerization of 2-benzyl-5-benzylidenecyclopentanone, a small increase in unit-cell volume was observed during a short initial period of time, which was then followed by a continuous decrease (Nakanishi *et al.*, 1980, 1981). For 5-benzylidene-2-(4-chlorobenzyl)cyclopentanone, a volume decrease from the beginning of the photodimerization could be seen (Turowska-Tyrk, 2003) and for 5-benzylidene-2-(4-bromobenzyl)cyclopentanone the unit-cell volume was constant during the entire reaction (Nakanishi *et al.*, 1981). It should be emphasized that Fig. 2 presents the dependence of the cell constants, not on irradiation time, but on product content, which is unusual in the scientific literature.

The changes in the cell constants for (I) are the result of changes occurring inside the unit cell. Figs. 3(*a*) and (*b*) present a product molecule (empty bonds) superimposed on a reactant molecule (filled bonds) for the initial stage of the photoreaction and for one of the final stages. It is very interesting that the C2 atom, belonging to the adamantane ring, shifted more significantly than the C11 atom during the creation of the new C2—C11 bond. For instance, for 4.4% reaction progress, the C2*P*···C2*R* and C11*P*···C11*R* distances (*P* and *R* represent the product and the reactant, respectively) are 1.08 (4) and 0.42 (4) Å, respectively. Certainly, the whole adamantane fragment changes its position in order to adapt to such a shift. The reason why the C2 atom, despite the fact that it is part of the adamantane fragment, moves to a greater degree can be rationalized in terms of the hydrogen bonds existing on the opposite side of the anionic chemical species. The system of hydrogen bonds is presented in Fig. 4. The carboxylate group forms hydrogen bonds with three ammonium ions. The hydrogen bonds anchor the $CO-C_6H_4-COO^-$ fragment and make its movement difficult. It should be added that these hydrogen bonds are not destroyed during the photoreaction. The mutual position of reactant and product is not constant during the photoreaction: the reactant and the product move relative to one another. This can be noticed by comparing Figs. 3(*a*) and (*b*). The change in position of the reactant and product with the photoreaction progress is presented in the deposited figure. This shift was monitored with the help of the C2*P*···C2*R* distance. The dependence is not linear: for a wide range the C2*P*···C2*R* distance is nearly constant and in the final stages it increases rapidly. (Note that

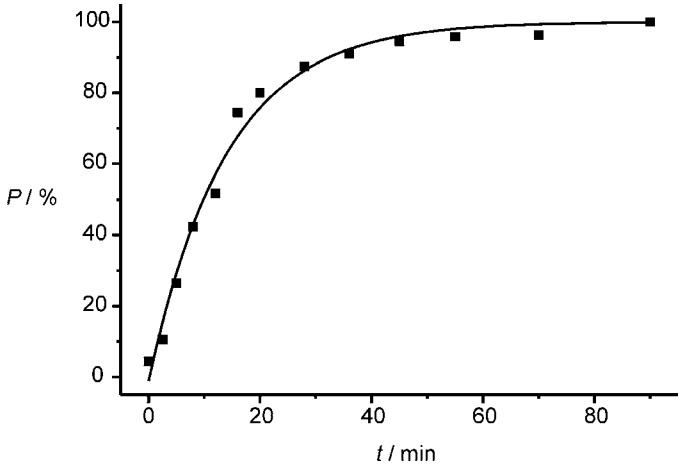

Figure 1
Relationship between the product content in a crystal and the time of irradiation. Standard uncertainties for the per cent of the product are in the range 0.0–1.0% with a mean value of 0.6%.

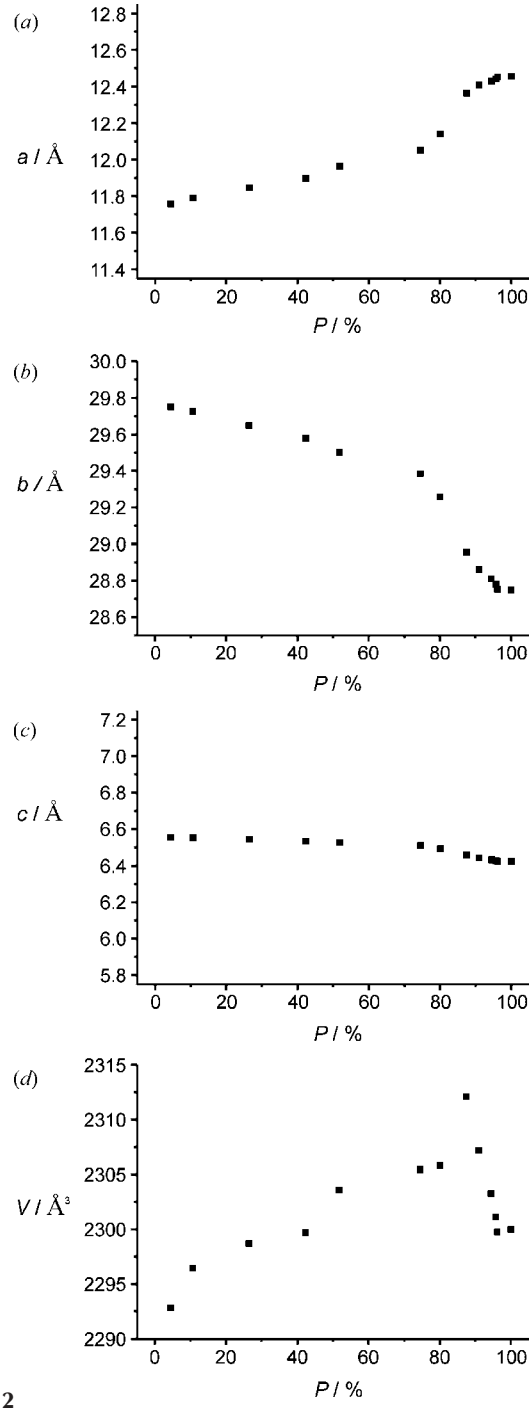

Figure 2
Variation in the cell constants and cell volume with the product content in a crystal. Standard uncertainties for *a*, *b* and *c* cell constants and the unit-cell volume are in the ranges 0.001–0.003, 0.002–0.006, 0.0005–0.0011 and 0.3–0.8 Å^3, respectively.

the analyzed distances refer to differences in positions averaged over the whole crystal.)

The molecular motions described above were not the only ones observed during the photoreaction. Fig. 5(*a*) presents the change in orientation of a fragment formed by atoms C10*R*, C11*R*, O1*R* and C12*R* (see Fig. 3 for atom labels). As can be seen, the angle between the above fragment and the *xy* plane is almost constant for most of the photoreaction, but changes quickly in the final stages. For the product species, we monitored the movements of the cyclobutane ring (C1*P*, C2*P*, C10*P*, C11*P*) formed in the photoreaction. We also observed a change in orientation of this fragment in the crystal. The results are presented in Fig. 5(*b*). The chemical species not taking direct part in the photoreaction, *i.e.* the C_6H–$CH(CH_3)NH_3^+$ cation, adapts to the changing orientation of the reacting anionic chemical species. Fig. 6 presents the relevant data. Figs. 5 and 6 indicate that the motions of the ions include a rotational component. Molecular movements

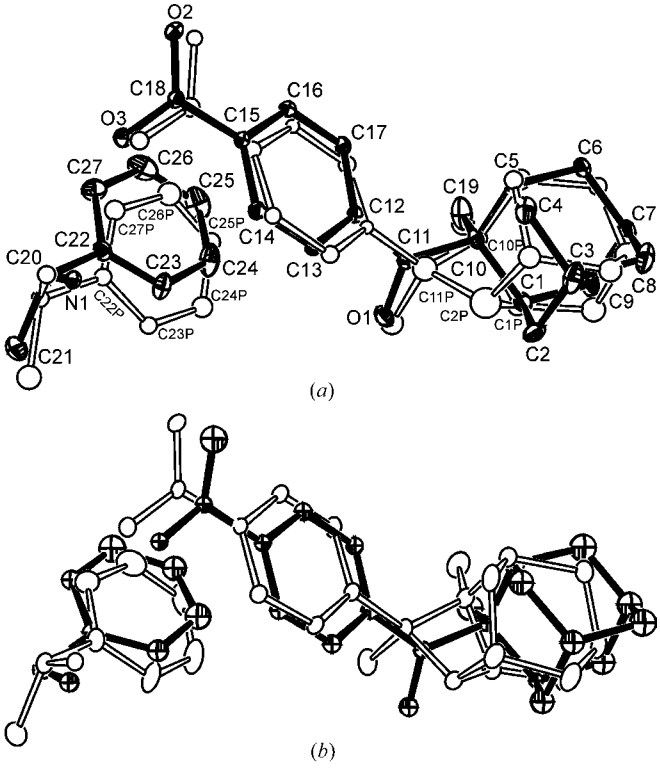

Figure 3
*ORTEP*3 (Farrugia, 1997) view of the product molecule (empty bonds) superimposed on the reactant molecule (filled bonds) for (*a*) the beginning stage of the photoreaction (4.4% of the product in a crystal) and (*b*) one of the final stages (94.5% of the product). H atoms were omitted for clarity. The projection of the molecules is on the same plane for both (*a*) and (*b*) parts of the figure. As can be seen, it was possible to separate all atoms of the reactant and product molecules. This was also possible for other reaction stages.

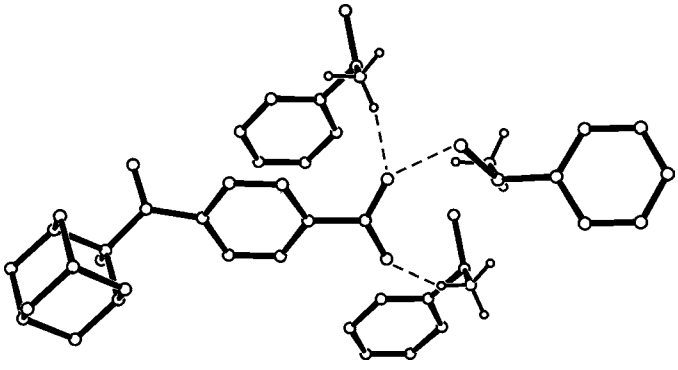

Figure 4
Hydrogen bonds created by the anionic chemical species.

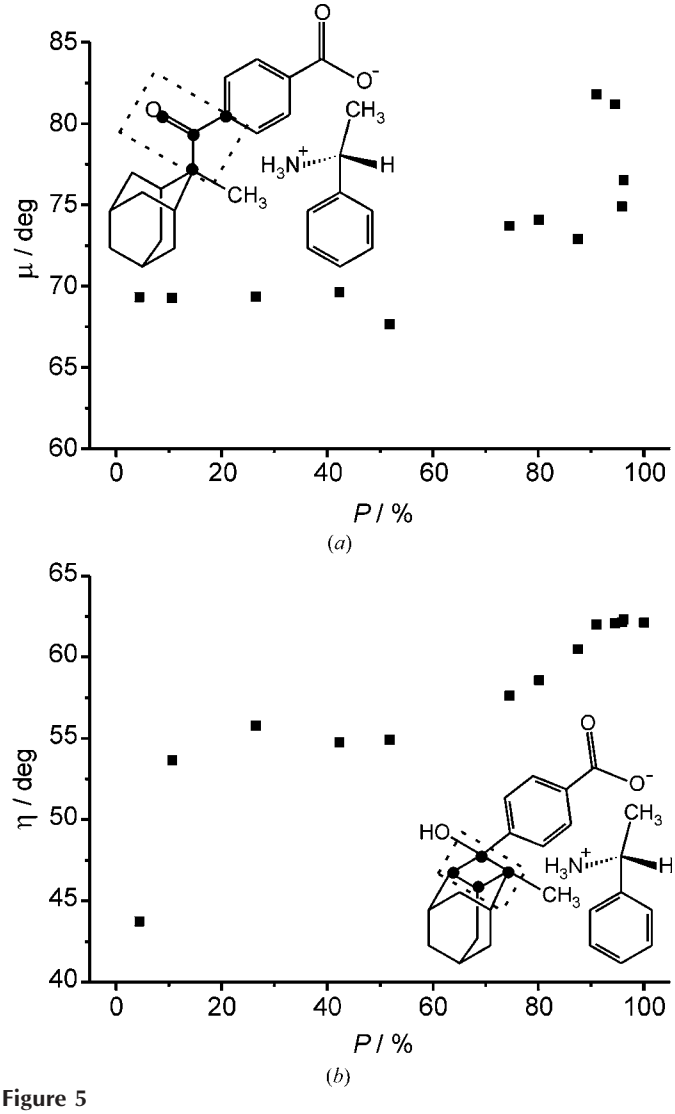

Figure 5
Variation in the angle between the plane formed by (*a*) atoms C10*R*, C11*R*, O1*R* and C12*R*, and (*b*) atoms C1*P*, C2*P*, C10*P* and C11*P* and the *xy* plane during the photoreaction. For better comparison the range of the axes was set to be the same. The C10*R*—C11*R*(O1*R*)—C12*R* fragment was chosen for monitoring purposes, because it is situated in the middle part of the reactant and should not be influenced strongly by intermolecular interactions. The C1*P*—C2*P*—C10*P*—C11*P* ring is the cyclobutane ring formed in the photoreaction. Standard uncertainties for μ and η are in the range 0.15–3 and 0.2–1.3°, respectively. The biggest changes in these parameters are 14.4 (3) and 18.6 (13)°, respectively, which indicates that they are statistically significant at the 3σ level, *i.e.* with 99.7% probability.

characterized by a rotational component were also observed for intermolecular reactions, namely [2 + 2] and [4 + 4] photodimerizations (Turowska-Tyrk, 2001, 2003, 2004; Turowska-Tyrk & Trzop, 2003).

Special attention was directed to the reaction center, namely to the atoms that form the cyclobutane ring in the photoreaction: C1*R*, C2*R*, C10*R* and C11*R*. Fig. 7(*a*) presents the change of the C2*R*—C1*R*—C10*R*—C11*R* torsion angle with the change in product content in the crystal. This angle changes very slightly in a crystal containing less than ∼ 80% of product molecules and increases significantly in the final stages of the photoreaction towards a value observed in the product molecule [−31.1 (3)° in the pure product crystal]. These data reveal the impact of the product molecules on the reactant: the product molecules force the reactant molecules to resemble the product. For the intramolecular reaction studied here such an effect is observed when the number of product molecules in a crystal is large. The influence of product molecules on the mutual orientation of reactant molecules was also seen for [2 + 2] and [4 + 4] photodimerizations (Fernandes & Levendis, 2004; Turowska-Tyrk, 2004). In the case of the photodimerization reactions, it was also observed that the distance between directly reacting atoms decreases with the photoreaction progress (Ohba & Ito, 2003; Turowska-Tyrk, 2001, 2003, 2004; Turowska-Tyrk & Trzop, 2003). The relationship between the C2*R*···C11*R* distance and reaction progress for the intramolecular reaction studied in this paper is presented in Fig. 7(*b*). The C2*R*···C11*R* distance is nearly constant during the majority of the reaction. This is not unexpected, since we are dealing with an intramolecular parameter that is harder to deform than an intermolecular one.

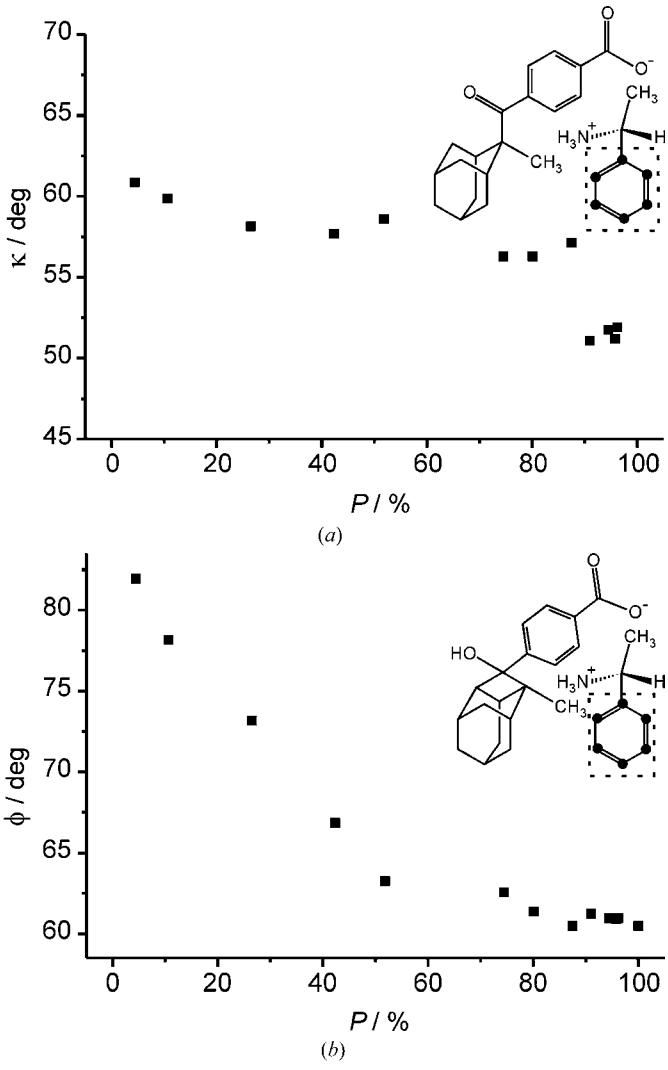

Figure 6
Variation in the angle between (*a*) the C22*R*–C27*R* and (*b*) the C22*P*–C27*P* benzene rings and the *xy* plane. For better comparison the range of the axes was set to be the same. Standard deviations for κ and ϕ are in the range 0.12–5 and 0.2–3°, respectively. The biggest changes in these parameters equal 10 (3) and 22 (3)°, respectively, which indicate that they are statistically significant at the 3σ level, *i.e.* with 99.7% probability.

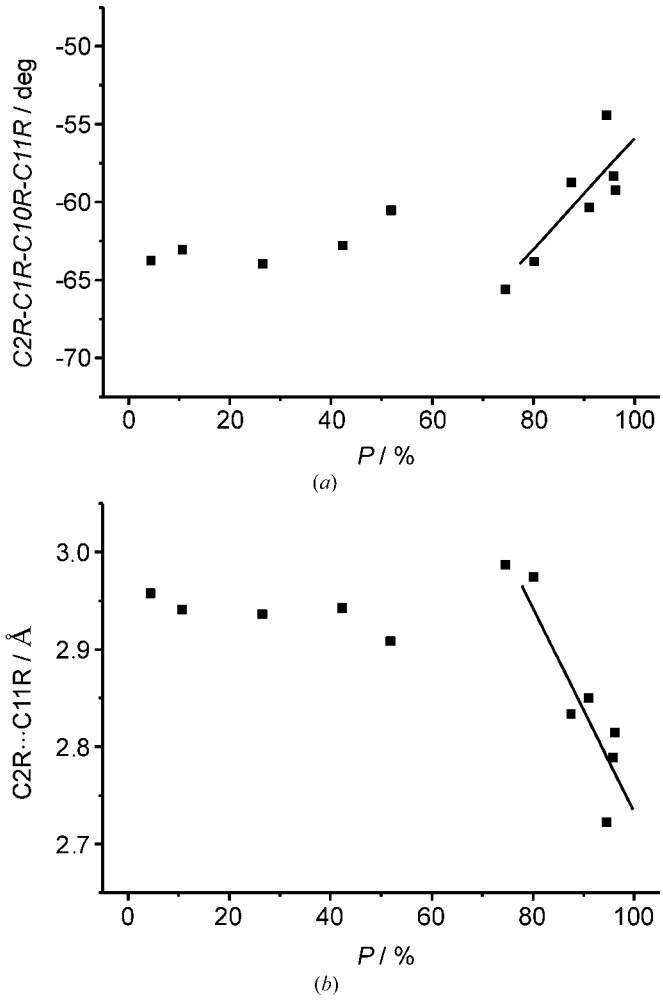

Figure 7
Relationship between (*a*) the C2*R*—C1*R*—C10*R*—C11*R* torsion angle and (*b*) the C2*R*···C11*R* distance and the product content in a crystal. Standard uncertainties for the torsion angle and the distance are in the range 0.4–4° and 0.006–0.08 Å, respectively. The biggest changes in these parameters are 12 (3)° and 0.27 (8) Å, respectively, which indicates that they are statistically significant at the 3σ level, *i.e.* with 99.7% probability.

4. Conclusions

Structural changes in a crystal during an intramolecular photochemical reaction, namely Yang photocyclization, were monitored as a function of reaction progress. The cell constants were found to change more rapidly during the final stages of the reaction, *i.e.* after $\sim 80\%$ product accumulation. Several features then change rapidly. Reactant and product molecules do not assume a fixed position during the photoreaction. They change their orientation in a crystal, but in the final stages of the photoreaction these changes occur more rapidly. The C2$R\cdots$C11R distance between directly reacting atoms is almost constant until $\sim 80\%$ reaction progress and afterwards decreases. The C2R—C1R—C10R—C11R torsion angle, consisting of reactant atoms that create the cyclobutane ring, is also nearly constant until about 80% reaction progress and afterwards increases toward a value observed for the cyclobutane ring in the product molecule. These observations are explained in terms of the influence of a large number of product molecules on a small number of reactant molecules. The adamantane fragment moves more than the remaining part of the anionic reactant species during reaction. This can be explained in terms of hydrogen bonding.

References

Boldyreva, E. V. (1999). *Reactivity in Molecular Solids*, edited by E. V. Boldyreva & V. Boldyrev, pp. 1–50. Chichester, New York, Weinheim: Wiley.

Farrugia, L. J. (1997). *J. Appl. Cryst.* **30**, 565.

Fernandes, M. A. & Levendis, D. C. (2004). *Acta Cryst.* B**60**, 315–324.

Harada, J., Uekusa, H. & Ohashi, Y. (1999). *J. Am. Chem. Soc.* **121**, 5809–5810.

Hosomi, H., Ohba, S., Tanaka, K. & Toda, F. (2000). *J. Am. Chem. Soc.* **122**, 1818–1819.

Kuma Diffraction (2000). *KM4CCD Software*, Version 166. Wrocław, Poland.

Leibovitch, M., Olovsson, G., Scheffer, J. R. & Trotter, J. (1997). *J. Am. Chem. Soc.* **119**, 1462–1463.

Leibovitch, M., Olovsson, G., Scheffer, J. R. & Trotter, J. (1998). *J. Am. Chem. Soc.* **120**, 12755–12769.

Nakanishi, H., Jones, W., Thomas, J. M., Hursthouse, M. B. & Motevalli, J. M. (1980). *J. Chem. Soc. Chem. Commun.* pp. 611–612.

Nakanishi, H., Jones, W., Thomas, J. M., Hursthouse, M. B. & Motevalli, J. M. (1981). *J. Phys. Chem.* **85**, 3636–3642.

Ohba, S., Hosomi, H., Tanaka, K., Miyamoto, H. & Toda F. (2000). *Bull. Chem. Soc. Jpn*, **73**, 2075–2085.

Ohba, S. & Ito Y. (2003). *Acta Cryst.* B**59**, 149–155.

Patrick, B. O., Scheffer, J. R. & Scott, C. (2003*a*). *Angew. Chem. Int. Ed.* **42**, 3775–3777.

Patrick, B. O., Scheffer, J. R. & Scott, C. (2003*b*). *Angew. Chem.* **115**, 3905–3907.

Scheidt, W. R. & Turowska-Tyrk, I. (1994). *Inorg. Chem.* **33**, 1314–1318.

Sheldrick, G. M. (1997). *SHELX*97. University of Göttingen, Germany.

Turowska-Tyrk, I. (2001). *Chem. Eur. J.* **7**, 3401–3405.

Turowska-Tyrk, I. (2003). *Acta Cryst.* B**59**, 670–675.

Turowska-Tyrk, I. (2004). *J. Phys. Org. Chem.* **17**, 837–847.

Turowska-Tyrk, I. & Trzop E. (2003). *Acta Cryst.* B**59**, 779–786.

Yamamoto, S., Matsuda, K. & Irie, M. (2003*a*). *Angew. Chem. Int. Ed.* **42**, 1636–1639.

Yamamoto, S., Matsuda, K. & Irie, M. (2003*b*). *Angew. Chem.* **115**, 1674–1677.